Adopting Data-Driven Safety Management Strategy for Thermal Runaway Risks of Electric Vehicles: Insights from an Experimental Scenario

applied sciences

MDPI

Article

Adopting Data-Driven Safety Management Strategy for Thermal Runaway Risks of Electric Vehicles: Insights from an Experimental Scenario

Huxiao Shi [1], Yunli Xu [2,*], Jia Qiu [2], Yang Xu [2], Cuicui Zheng [2], Jie Geng [1], Davide Fissore [1] and Micaela Demichela [1]

[1] Department of Applied Science and Technology, Politecnico di Torino, 10129 Turin, Italy; huxiao.shi@polito.it (H.S.); jie.geng@polito.it (J.G.); davide.fissore@polito.it (D.F.); micaela.demichela@polito.it (M.D.)
[2] Zhejiang Key Laboratory of Consumer Product Safety Research Under Provincial Market Supervision, Zhejiang Institute of Quality Science, Hangzhou 310018, China; qiuj@zjiqs.cn (J.Q.); xuy@zjiqs.cn (Y.X.); zhengcc@zjiqs.cn (C.Z.)
* Correspondence: xuyl@zjiqs.cn

Abstract

Thermal runaway (TR) of lithium-ion batteries (LIBs) represents a critical safety challenge in EV applications. This study explores the potential of data-driven safety management strategies for mitigating TR risks in EVs. To minimize the impact of external environmental factors on the degradation of LIBs, experiments were conducted using an accelerating rate calorimeter (ARC). The intrinsic thermal behavior of six nickel–cobalt–manganese (NCM) cells at different states of health (SOH) and operating temperatures has been captured in created adiabatic conditions. Multiple sensors were deployed to monitor the temperature and electrochemical and environmental parameters throughout the degradation process until TR occurred. The results show that both the thermal and electrochemical stability of LIBs have been affected, exhibiting consistent thermal patterns and early electrochemical instability. Furthermore, even under adiabatic conditions, the degradation of LIBs show synergistic effects with environmental parameters such as chamber temperature and pressure. Correlation analysis further revealed the coupling relationships between the monitored parameters. Through calculating their correlation coefficients, the results indicate advantages of combining thermal, electrochemical, and environmental parameters as being to characterize the degradation of LIBs and enhance the identification of TR precursors. These findings stress the importance of considering the battery-environment system as a whole in safety management of EVs. They also provide insights into the development of data-driven safety management strategies, highlighting the potential for achievement and integration of anomaly detection, diagnosis, and prognostics functions in current EV management frameworks.

Keywords: electric vehicles; lithium-ion battery; thermal runaway; safety management; data-driven analysis

Academic Editor: Ján Dižo

Received: 21 November 2025
Revised: 13 January 2026
Accepted: 14 January 2026
Published: 19 January 2026

1. Introduction

Battery safety is becoming more and more critical with the rapid diffusion of electric vehicles (EVs). Having the advantages of high energy and power density, long cycle life, and fast charging capability compared with other devices, lithium-ion batteries (LIBs) are

widely used in EVs [1–3]. Due to the closed structure of LIBs and flammable internal materials, their use introduces additional hazards to EVs, by increasing combustion and explosion risks [4]. Thermal runaway (TR) of LIBs is typically the root cause of EVs' combustion accidents, and it can happen at different conditions [5]. TR can be caused by thermal, electrical, and mechanical abuse, like excessive heat, rapid charge/discharge cycles, or physical damage [6]. Once abuse exceeds the tolerance range, internal reactions trigger the rapid generation and accumulation of significant heat and gas, likely causing combustion and explosion in an airy atmosphere [6,7]. TR also poses severe chemical hazards to both humans and the environment due to potentially released toxic gases [8]. For more discussion on the mechanisms and hazards of TR of LIBs, please refer to [9–11]. Given these severe risks, effective safety management of EVs to prevent TR is crucial.

Implementing effective safety management for EVs faces multiple challenges. These challenges arise not only from the intrinsic characteristics of LIBs themselves but also from the complex system design and operational conditions of EVs. Firstly, to ensure battery safety, more stringent requirements are placed on the operation of LIBs. According to Deng et al. [12], LIBs must operate within a relatively narrow temperature and voltage window. Previous studies have generally suggested that the ideal temperature range for safe LIB operation lies between 25 and 40 °C, with tolerances of approximately ±5 °C [13–15]. Though the maximum operating temperature could reach 60 °C according to some studies [16], this evidence limits the reliability and applicability of EVs, making them difficult to adapt to changing environments. Secondly, the transition from LIBs TR to fire ignition on EVs occurs within an extremely short time window. According to the experimental results of Yin et al. [17], it takes around 13 min for the battery pack to pass from the smoke generation stage to the combustion stage, followed by an additional 2 min to reach the stage of complete vehicle combustion. The short time window increases the difficulty of the effective preventive actions. Though practical situations may vary as the experiment was in a confined garage, these data highlight that during the entire process of TR propagation until the combustion, the driver and passengers do not have much time to react and escape. More importantly, this research also points out that the overall temperature change in the vehicle was relatively small before the stage of battery pack combustion, making early detection of TR signs difficult through human perception alone. Moreover, the energy supply of EVs relies on battery packs rather than individual cells, which significantly increases the system complexity. Once TR occurs in a single cell, the high temperature and combustion phenomenon can propagate to adjacent cells, leading to the larger scale TR for the whole battery pack with more severe safety consequences [18,19]. Given these challenges, developing effective EV safety management strategies requires considering practical factors across prevention, early warning, emergency response, and post-disaster rescue phases. Considering the extremely short time window between the onset of TR and combustion, early warning becomes especially vital, as it provides the last opportunity to intervene before the TR escalates into uncontrollable accidents with severe consequences.

Given the high complexity brought about by LIBs themselves and the actual operating scenarios of EVs, data-driven approaches have shown their potential for safety modeling and developing safety management strategies for EVs. Recently, researchers have broadly adopted data-driven methods to study the thermal behavior of LIBs, aiming to leverage operational data to predict TR triggering and propagation, while also supporting a shift in safety management from passive reactive approaches to proactive early warning systems [20,21]. Operational data can be obtained from either real-world scenarios or laboratories, including historical accident data and real-time monitored data [22,23]. Data fusion appears promising, provided that sufficient high-quality data are available. By

conducting multi-parameter monitoring, multi-dimensional signals from diverse sensors can enhance the robustness of safety models, with the advantage of accurately characterizing TR scenarios [21,24]. At the same time, researchers also pointed out the limitations of relying solely on laboratory experiments or historical accident data, where potential TR events may not be comprehensively captured [25]. Real-world operational data may provide a solution to this limitation. As demonstrated in [5], operational data for EVs support better capture the dynamic characteristics of LIBs in practical scenarios, which can be utilized to forecast failure risk and alert anomalies. However, one concern of utilizing real-world operational data is the impacts from external environments, which is, as previously discussed, potentially due to the sensitivity of LIBs to the operating temperature and other environmental factors.

In this study, the potential of implementing data-driven strategies in safety management for EVs regarding TR risks has been investigated and discussed through a designed experiment. To minimize the impacts from external environmental factors, an accelerating rate calorimeter (ARC) is adopted to capture the intrinsic thermal behavior of LIBs through creating adiabatic conditions. The degradation to TR occurrence evolution of LIBs can be reflected by the monitored multi-parameters. Unlike conventional ARC-based studies that primarily focus on temperature profiles, this work adopts a data-driven perspective by integrating thermal, electrochemical, and environmental signals through multiple sensor measurements. The objective is not only to describe TR evolution, but also to explore intrinsic degradation patterns and early precursors that can provide valuable insights for conducting data-driven safety management on EVs. This paper is organized as follows. Section 2 introduces the current safety management methods for EVs as well as ARC-based research. Section 3 demonstrates the designed experiment and results. At the end, discussions and conclusions are provided in Sections 4 and 5.

2. State of the Art

This section reviews the current state of the art related to safety management and experimental investigations of TR in EVs and LIBs. The section is structured into two parts: Section 2.1 reviews the existing safety management methods mitigating TR risks in EV applications, and Section 2.2 discusses ARC-based experimental studies focusing on TR of LIBs.

2.1. Current Safety Management Methods for TR of EVs

Ensuring the thermal and electrochemical stabilities of LIBs is a key focus in battery safety management of EVs, whose goal is to guarantee EVs' normal operation, especially in abuse conditions. To cope with thermal abuse, methods in both passive and proactive manners are currently adopted in practice.

At the design stage of EVs, the preventive design is emphasized to suppress or delay the occurrence and propagation of TR through materials, structures, and protection designs. Safety devices such as safety vents, thermal fuses, and shutdown separators act as critical barriers that can quickly release internal pressure, cut off current paths, or block heat transfer under abnormal circumstances, thereby preventing TR chain reactions caused by gas accumulation, overheating, or short circuits inside cells [12,26]. On the other hand, the limited adaptability of passive safety management methods to complex operation scenarios places higher demands on proactive safety management methods. A battery management system (BMS), in this case, has been widely adopted in EVs to perform monitoring, controlling, optimizing, and safety insurance from massive hazards [27]. Through monitoring temperature, voltage, and other characteristics of batteries using deployed sensors, BMS supports the EV to achieve functions of state estimation (e.g., state of charge, stage of health,

etc.), cell balancing toward their different states in various configurations for battery packs, anomaly detection and diagnosis when the LIBs operate beyond their normal operating window, and corresponding control actions once an anomaly has been detected [28–30].

Effective thermal monitoring enhances the performance of the battery thermal management system (BTMS). To maintain the thermal stability of battery packs, BTMSs must provide both heating and cooling capabilities under extreme operating conditions [31,32]. With recent advancements in air, liquid, phase change material, and heat-pipe-based cooling techniques, BTMS has gained increasing attention in TR-related safety management scenarios [33]. However, the performance of BTMS largely relies on its coordination with BMS, since actions are taken upon the detected temperature anomalies under the control of an electronic control unit in BMS [34]. As discussed in several studies, BMS is limited to guarantee battery safety toward TR risks. Being categorized as one of TR's early warning technologies for LIBs, BMS widely adopts threshold analysis to diagnose anomalies or faults. The presence of a fault is determined by the predefined parameter boundaries, such as temperature and voltage [28]. However, one main challenge of this approach is to set appropriate thresholds. LIBs show various thermal behaviors under different operation conditions, and it is thus difficult to define universally effective thresholds, which hinders the accuracy and reliability of such approaches [35]. At the same time, BMS can only measure the surface temperature, terminal voltage, and terminal current, usually resulting in a slow response [7]. Experiences from many cases have shown that the significant abnormality has already occurred by the time the alarm is triggered by the temperature signal [35]. In addition, complex internal principles, uncertain working conditions, and environmental factors further hinder the reliability of BMS-based thermal monitoring [30,36].

Overall, while the BMS and BTMS provide fundamental thermal protection, their responses are relatively reactive and occur only after critical thresholds are exceeded. These limitations highlight the need for more advanced approaches to detect early-stage anomalies of TR, enabling the implementation of safety management strategies based on proactive prediction.

2.2. ARC-Based Research Toward TR of LIBs

As an important method to study the thermal behavior of materials, the ARC allows for us to provide an adiabatic environment, which limited the heat exchange between LIBs and outsiders during the self-production heat phase [37,38]. ARC experiments are always conducted to study battery stability, including TR temperatures and battery characteristics [39]. The ARC device comprises a closed chamber and a control system. Samples are placed in the chamber and a TR is triggered. The control system is responsible for controlling the temperature of the chamber wall and recording the temperature changes in the measurement points on the sample surface. In the research, ARC supports the evaluation of the thermal safety of LIBs under thermal abuse. Zhang et al. [40] studied the adiabatic thermal behavior of solid–liquid hybrid electrolyte LIBs in 50% and 100% state of charge (SOC) levels, where the self-heating onset temperature (T_{onset}), thermal runaway triggering temperature (T_{tr}), maximum temperature in thermal runaway (T_{max}), and the temperature rise rate (dT/dt) recorded from the ARC were applied as safety evaluation indicators. Liu et al. [41] adopted ARC with an instilled pressure transducer to obtain the profile of critical temperature and pressure for cylindrical LIBs, testing the fire suppression performance of typical fluorinated immersion cooling agents. Kim and Lee [42] investigated the fire characteristics of LIBs with three SOCs (0%, 50%, and 100%) through ARC; it was found that the fire risk index of the LIB with 100% SOC is much higher than that with 50% SOC, and there was no explosion for 0% SOC. Overall, ARC shows great universality in LIBs multilevel safety evaluation, and thus has widely been adopted in LIBs thermal safety

management [43]. However, most of this work only focused on the temperature profiles of LIBs, or highlighted the importance of static parameters, like peak temperature, onset temperature, maximum temperature rise rate, etc. A perspective beyond the temperature focus is called for, by considering synergistic approaches among ARC and other devices [44]. In addition, though some ARC-based studies have discussed the influence of the SOC on the TR behavior of LIBs, further factors still need to be considered, such as variations in the state of health (SOH), working conditions (especially operating temperatures), etc. Lastly, ARC-related research is often subjected to the relatively small amount of experimental data available and the restricted LIBs format that is allowed to be tested. This may be due to the high cost of ARC experiments and constraints imposed by the chamber size. As discussed in [43,45], except adopting the extended volume-ARC (EV-ARC), only a narrow range of LIB formats can be supported by standard ARC setups, usually with lower capacities.

3. Experiment Design and Results

This section presents the experiment design and the corresponding results of this study. To investigate the intrinsic thermal behavior of LIBs under controlled conditions, Section 3.1 introduces the experiment design, followed by the presentation of results obtained from the ARC-based tests (Section 3.2).

3.1. Experiment Design

To illustrate the designed experimental scenario, Section 3.1.1 introduces the selected samples, including their characteristics, experimental conditions, and the description of datasets obtained. Section 3.1.2 describes the experimental setup, including the ARC system specifications, the measurement and data acquisition configuration, and the experimental procedure adopted to characterize the TR behavior of the tested samples.

3.1.1. Sample Selection

Six nickel–cobalt–manganese (NCM) cells have been selected as samples in experiments. The size is 7.3 × 91.0 × 186.0 mm, the nominal capacity is 16 Ah, the nominal voltage is 3.7 V, and each weight is approximately 279 g. Considering that the LIBs capacity used in EVs is generally large, this experiment selected large-capacity LIBs as much as possible within the range allowed by the chamber.

Previous studies [13–15] have generally suggested that the ideal temperature range for safe LIB operation lies between 25 and 40 °C. Following the steps of the cycling test by using a constant current–constant voltage (CC–CV) protocol (a constant current of 1.0 C was firstly applied until the cell voltage reached 4.20 V, followed by constant-voltage charging at 4.20 V until the current decreased to 0.05 C), six experimental batteries were obtained at three states of health (SOH 100%, 95%, 85%) under two operating temperature levels, where 25 °C represents the normal operating temperature condition of NT and 45 °C represents the high operating temperature condition of HT. SOH can be calculated through the ratio of the current capacity of LIBs and its initial capacity [28]. Each SOH–temperature combination is represented by a single cell. Therefore, experimental results can reflect cells' degradation patterns. All these six samples were further tested through ARC experiments, resulting in six datasets.

3.1.2. Experimental Setup

The ARC used in the experiment is manufactured by HEL Ltd. (UK), with the series number of BTC-500. The equipment has a chamber with a diameter of 500 mm and a volume of 98 L. The range of accepted temperatures for testing is from −20 to 300 °C, and the range of pressure is from 1 to 4 bar. The equipment records measurements of temperature-related parameters, electrochemical parameters of the sample, and parameters

related to the performance of the chamber (see in Table 1). Most parameters can be directly measured in situ by the ARC, and the sensor accuracy is provided in Table 1. To guarantee the synchronization of parameters, all measurement channels were acquired through a centralized data acquisition system operating at a maximum sampling rate of 10,000 Hz, which ensured near-simultaneous recording of the temperature, pressure, and electrical signals.

Table 1. The parameters monitored in the experiment.

Parameter	Interpretation	Accuracy
Time (min)	Time recorded in experiment, where 0 min represents the moment when self-heating occurs (reaching the exothermic sensitivity threshold: 0.02 °C/min).	-
Sample Temperature (°C)	Sample temperature, the expectation value of measurements from two deployed thermocouples.	±0.05–0.1 °C
Chamber Temperature (°C)	Chamber temperature, measured at the side wall of the chamber.	±0.1 °C
Vessel Pressure (bar)	Pressure in the chamber.	±0.1–0.25% of full scale (FS)
Sample ROC (°C/min)	Rate of change in sample temperature, calculated every 5 min by calculating the temperature difference between two continuous measurements and dividing it by the corresponding time interval.	-
Sample Self-Heat (°C)	Temperature rise caused by spontaneous heating of the sample.	-
Chamber Heating Power (%)	Relative heating power at the side wall of the chamber, expressed as a percentage of its maximum rated power (4000 W).	Within ±1%
Sample Voltage (V)	Voltage of the sample.	±0.01–0.05% FS
Sample Internal Resistance (Ω)	Internal resistance of the sample.	-

The sample (Figure 1) was placed in the middle of the adiabatic chamber of the ARC. During the experiment, the Heat–Wait–Search (HWS) mode had been adopted to detect spontaneous heat generation at each increment of the temperature. Starting from room temperature, there was a temperature increase of 5 °C for each heating phase, which was followed by a waiting phase. A thermal equilibrium was created in this phase between the temperature of the chamber and that of the sample. To reduce the waiting time, the implemented heating wires were controlled by the control system to heat the sample uniformly. At the end of this phase, exothermic self-heating was sought in the searching phase, and a new HWS cycle began if no significant self-heating was detected. The sensitivity threshold value of ARC was set as 0.02 °C/min, where the calorimeter switched to exothermic control mode once the exothermic self-heating of the sample reached this threshold [46]. An adiabatic condition without heat transfer to an external environment was established in this phase, where samples' subsequent self-heating was able to reflect their intrinsic thermal behavior. The explosion occurred soon after the occurrence of TR (Figure 1), leading to

the maximum temperature, and then the cooling phase began with a sharp decrease in the temperature.

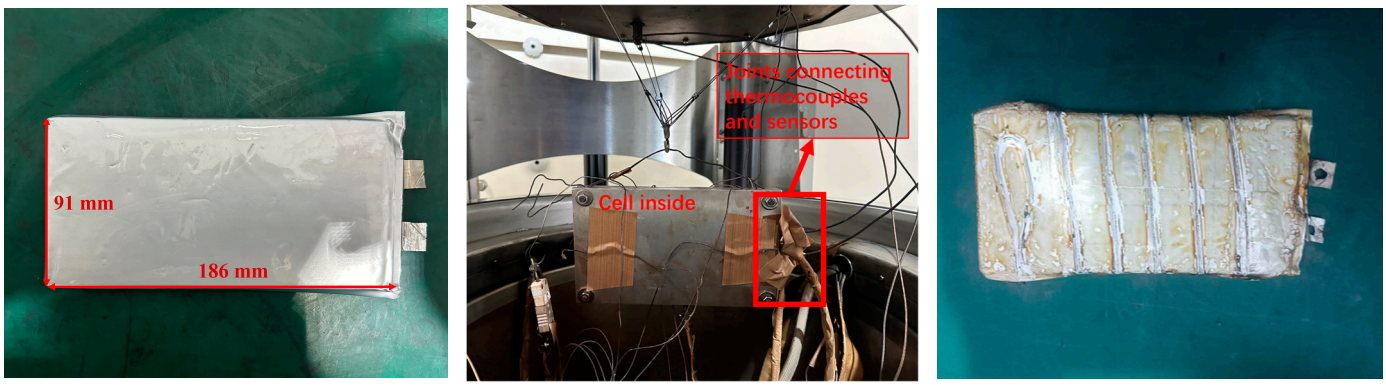

(**a**) (**b**) (**c**)

Figure 1. (**a**) The sample before the experiments; (**b**) the sample implemented in the ARC chamber; and (**c**) the sample after the experiments with the occurrence of TR.

3.2. Experiment Results

Figure 2 displays the intrinsic thermal behavior of the sample NT-100% through three phases in the experiment: the HWS phase, the self-heating phase, and the cooling phase. To reflect the degradation behavior of LIBs in adiabatic conditions, their performances in the self-heating phase (orange zone in Figure 2) are concentrated in this section. The dynamic measurements of different parameters from the moment of self-heating onset (t_{onset}) to that of the maximum temperature (t_{maxT}) for six samples were analyzed.

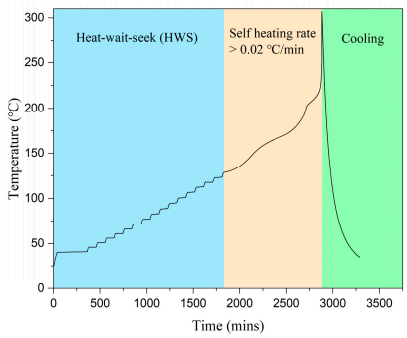

Figure 2. The intrinsic thermal behavior of the sample NT-100%.

Figure 3 displays the trends of temperature-related parameters during experiments for all samples, where red dots represent t_{TR}. Regarding the results, the sample surface temperature and chamber temperature showed a highly consistent evolution trend (Figure 3a,b). This result is reasonable: during the experiment, the temperature of samples increased due to self-heating (Figure 3c), while the ARC dynamically adjusted the chamber temperature to create an adiabatic condition that met the experimental requirements. However, the chamber temperature was generally 20 to 40 °C higher than the sample temperature.

Critical temperature parameters of samples recorded in the experiment have also been shown in Table 2. Specifically, the sample temperature was mainly concentrated between 120 and 130 °C at t_{onset}, with the lowest temperature being shown by NT-85% (approximately 106 °C). The sample temperature showed a relatively linear increasing trend (Figure 3a). At t_{TR}, the sample temperature was concentrated around 230 °C, followed by a continuous increase above 300 °C. HT-95% displays the maximum temperature, with the figure of 341 °C. This phenomenon occurred within 10 min for all samples. In detail, the shortest was only 5 min (NT-85%), followed by HT-95% (5.3 min), NT-95% (7.8 min),

HT-100% (8.2 min), HT-85% (8.3 min), and NT-100% (9.7 min). Figure 3d displays the rate of change in the sample temperature, calculated every 5 min. The peak due to a sharp increase has been shown for all samples before t_{TR}, indicating that all samples experienced a period of rapid temperature rise before thermal runaway was triggered. Such a phenomenon occurred for each sample at moments around 826 min (NT-100%), 881 min (NT-95%), 1436 min (NT-85%), 826 min (HT-100%), 821 min (HT-95%), and 971 min (HT-85%) after t_{onset}.

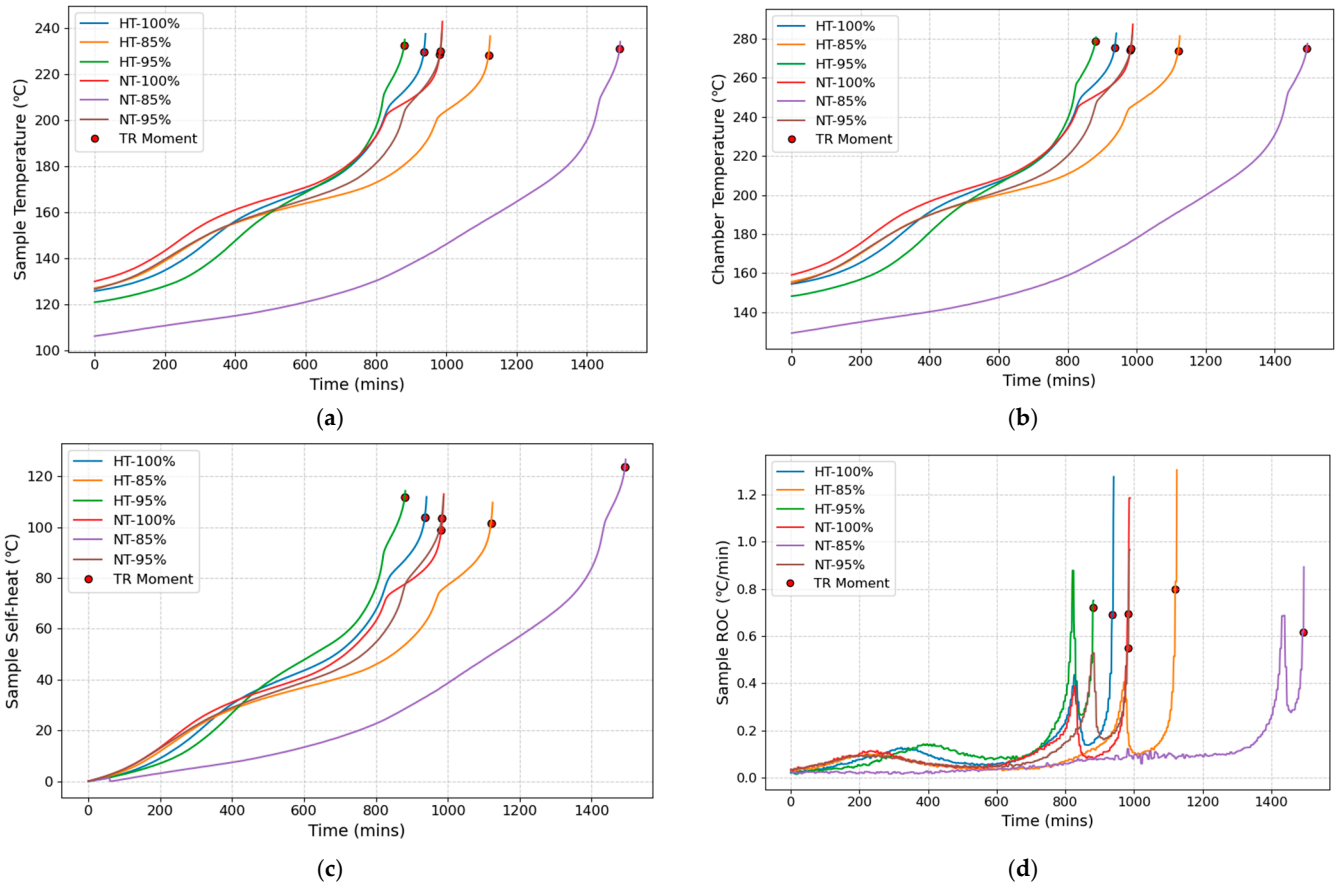

Figure 3. Trends of temperature-related parameters for the following: (**a**) sample temperature; (**b**) chamber temperature; (**c**) temperature rise caused by spontaneous heating of the sample; and (**d**) rate of change in sample temperature calculated every 5 min. In the legends, "NT–X%" and "HT–X%" denote operation at normal temperature (25 °C) and high temperature (45 °C), respectively, with X% representing the SOH level of the cell.

Table 2. Critical temperature parameters for samples recorded in experiments.

Sample	T_{onset} (°C)	T_{tr} (°C)	T_{max} (°C)
NT-100%	130.0	228.6	306.9
NT-95%	126.6	230.0	335.3
NT-85%	106.1	230.8	329.6
HT-100%	125.9	229.6	323.0
HT-95%	120.9	232.6	341.1
HT-85%	127.0	228.2	317.5

Figure 4a presents the evolution of the chamber pressure for different samples. A similar trend is shown, starting from a relatively stable stage, followed by an increasing

trend. As the temperature rises due to self-heating reactions, the pressure gradually increases due to gas release from electrolyte decomposition and internal venting. Once the TR has been triggered, a rapid pressure spike can be observed, corresponding to strong exothermic reactions and a massive gas release. In addition, a higher pressure level occurred overall for samples that operated in the high-temperature operating condition (45 °C), indicating that the internal reactions and TR of LIBs tended to release a larger amount of gas under high-temperature operating conditions. Figure 4b presents the evolution of the chamber heating power, which implies the change in the amount of heat compensation required for the chamber to maintain an isothermal state. With an increase in sample temperature, the chamber increases its heating power. A pronounced peak can be observed before t_{TR}, showing a strong consistency with the behavior of 'Sample ROC'. The coincidence of the timing (NT-100%: 825 min; NT-95%: 878 min; NT-85%: 1435 min; HT-100%: 826 min; HT-95%: 820 min; HT-85%: 968 min) further validates the experimental findings, and also implies the synergistic effect between the sample and the chamber. Comparing the evolution of the sample internal resistance (Figure 4c) and voltage (Figure 4d), the internal resistance of all samples shows a clearer pattern, with abrupt changes occurring early in the self-heating stage. Such a phenomenon can be regarded as a precursor to TR in LIBs, thus supporting an early warning during their self-heating phases.

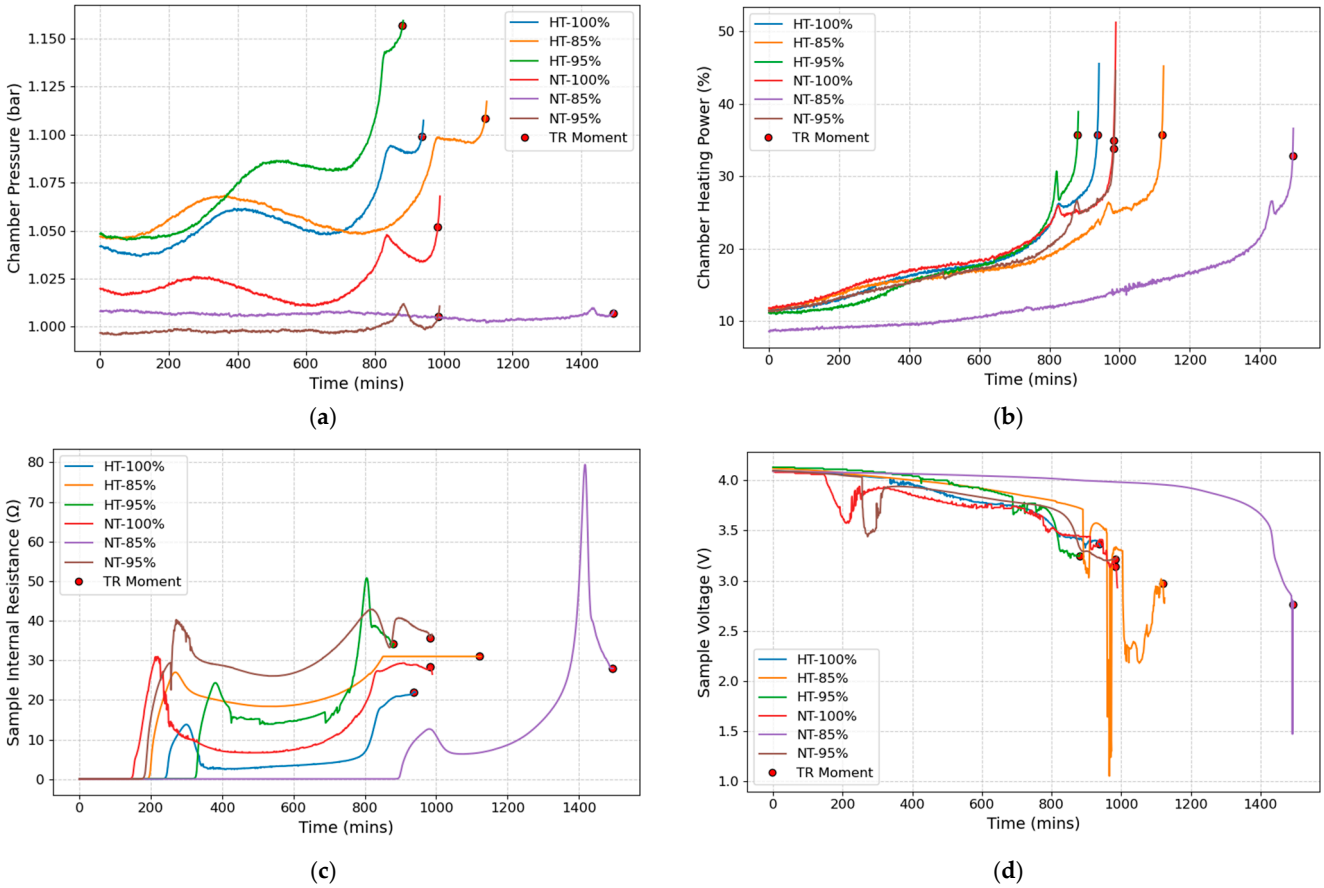

Figure 4. Trends of chamber-related parameters and electrochemical-related parameters for the following: (**a**) chamber pressure; (**b**) chamber heating power; (**c**) sample internal resistance; and (**d**) sample voltage.

To quantitatively explore the relationships between the monitored parameters, a correlation analysis was conducted using Pearson correlation coefficients. Figure 5 displays the constructed correlation heatmap, where the color intensity represents the magnitude of the Pearson correlation coefficient r.

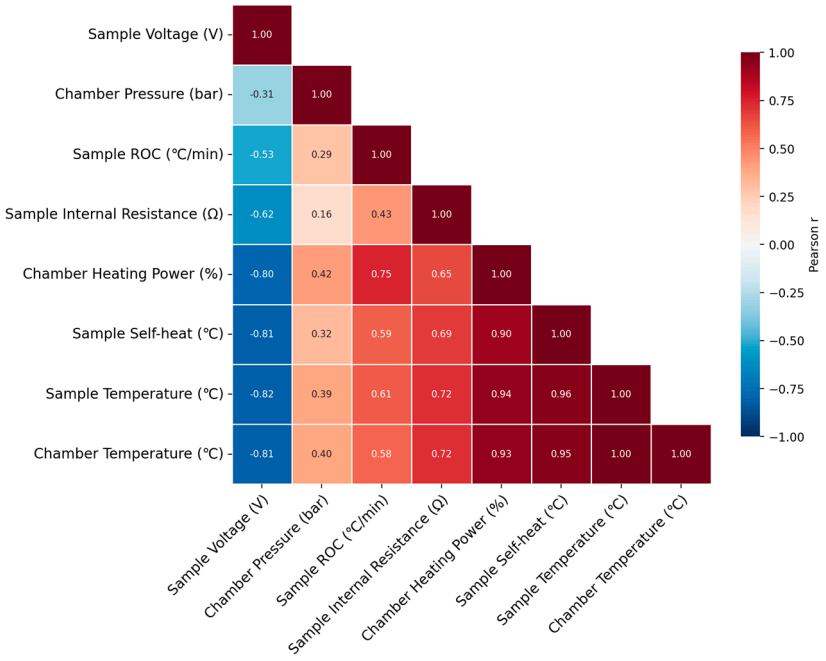

Figure 5. Correlation heatmap constructed from monitored parameters.

As for the result, parameters like 'Chamber Heating Power', 'Sample Self-Heat', 'Sample Temperature,' and 'Chamber Temperature' show strong correlations with each other (with high absolute *r* values), and a high correlation level with 'Sample Internal Resistance'. 'Sample ROC' shows high correlation with 'Chamber Heating Power,' which further validates the previous finding, according to the trend analysis. In addition, 'Sample Voltage' shows a strong negative correlation with other parameters, indicating that the voltage drop is closely associated with the heat generation and thermal instability of LIBs. Compared with other parameters, 'Chamber Pressure' has a lower correlation with other parameters throughout the whole period. However, the characteristics shown through its trend (Figure 4a) exhibit greater consistency with other parameters (such as 'Sample ROC' and 'Chamber Heating Power'), which all exhibit a peak in the stage approaching TR due to its sharp increase. These results further reveal the coupled relationships among the parameters monitored in the experiments, including not only the temperature and electrochemical parameters of the LIBs, but also environmental variables that are related to the chamber.

4. Discussion

In the experiment design of this study, the experiment minimizes the impacts from external environmental factors in the degradation of LIBs. By selecting six experimental samples at different SOH and operating temperature levels, the reliability and representativeness of the research results are expected to be guaranteed. These samples have a relatively large nominal capacity (16 Ah) for studies using ARC, which enhances the relevance of the experimental results to practical scenarios. In the experiment, the samples underwent a self-heating process until the occurrence of TR, with multiple sensors being used to monitor eight parameters. The performances of these parameters benefit, revealing the main characteristics of LIBs in their degradation.

According to the results, both the thermal stability and electrochemical stability of LIBs were significantly affected during their degradation process. Though they vary in SOH and operating temperature levels, similar patterns have been observed among all samples. The surface temperature exhibits a higher and higher increasing trend, with

a sudden and sharp increase in the rate of change near the TR stage. Electrochemical parameters tend to be become unstable, which is reflected by the overall increase in internal resistance and the decrease in voltage, both exhibiting increasing volatility levels. Besides changes in the performance of the LIBs themselves, environmental parameters are also relevant. Even in adiabatic conditions where external influences are largely minimized, the thermal behavior of LIBs during degradation still exhibits a synergistic response with its surrounding environment, which is reflected by the temperature and pressure of the chamber. Moreover, the coupling relationships among the monitored parameters were revealed, suggesting that TR in LIBs can be indicated synergistically by comprehensively considering the thermal and electrochemical behavior of batteries and their interactions with the surrounding environment.

These findings are beneficial for developing data-driven safety management strategies for EVs TR risks. Firstly, the effectiveness of data-driven strategies to identify TR precursors has been validated. By deploying sensors to monitor battery performance and its interaction with the surrounding environment, the key characteristics of the relevant parameters can be used as precursors, which can support effective diagnostics and decision-making, and thus contribute to the health management of EVs in response to TR risks.

The results also demonstrate that focusing solely on critical temperature parameters (such as self-heating onset temperature, TR triggering temperature, and maximum temperature in TR) has limitations in characterizing the overall degradation trend of LIBs. During the experiments, temperature-related parameters showed an accelerating and smooth increase, without any obvious signatures (e.g., abrupt changes, increased volatility, etc.). This increases the difficulty of early TR warnings based on single-point temperature monitoring. However, the consistent intrinsic thermal behavior pattern followed by LIBs implies the possibility of enabling health-state estimation through dynamic monitoring of the temperature parameters. Based on the similarity of these trends, the remaining operating time before TR during the self-heating phase can be predicted, providing valuable support for EV battery safety management.

Moreover, the electrochemical properties of the battery demonstrate a crucial role in early warnings for TR. During the self-heating phase, electrochemical instability appears at the early stage, which means that early anomalies in these parameters can effectively be used to define early warning points. In addition, this study preliminarily validates the interaction between the battery and its surrounding environment, implying the necessity of evaluating the LIBs-environment system from a system-level perspective. Correlation analysis further confirms this point; the high correlation between parameters reveals their synergistic effects in the degradation of LIBs. This perspective is significant for the safety management of EVs, as their actual operating conditions are not static. Thus, to develop effective safety management strategies to mitigate TR risks, especially developing reliable and applicable early warning technologies for EVs, it is necessary to consider not only the thermal and electrochemical stability of LIBs but also the overall performance of the entire system. In this context, the degradation of LIBs in adiabatic conditions can be regarded as an intrinsic reference benchmark, representing battery responses without external environmental disturbances. By dynamically identifying and evaluating deviations induced by different operating conditions, this benchmark shows potential to inform data-driven anomaly detection and early warning algorithms in BMS/BTMS in real applications. For example, temperature-related parameters can be used to characterize the overall degradation trend of LIBs, as their evolution typically exhibits relative linear behavior. Electrochemical parameters such as internal resistance and voltage are more sensitive to early-stage instability and abrupt changes, showing their potential for being early warning and anomaly detection indicators. Finally, to support decision-making, combining results

from different perspectives in this study allows us to provide a comprehensive evaluation of the health state of LIBs on EVs, and thus supports taking different actions in terms of different TR risks.

The limitations of this study come from the following aspects. The first limitation relates to the small sample size. Due to the high complexity and expense of the conducted experiments, the availability of the experimental results was limited, hindering the data acquisition and database establishment. As a result, variability among individual samples could not be systematically quantified. Although the initial conditions of samples were differentiated through considering different SOH and operating temperature levels, the corresponding behavior differences were not discussed in detail in this study. Instead, the study focused on the similarities between cells across different conditions to explore the consistent degradation pattern and key characteristics related to TR. One condition represented by a single cell limited the statistical evaluation for result variability and reliability. To further validate the effectiveness of data-driven solutions in the safety management of EVs, it is meaningful to expand the sample size by conducting more experiments, including repeated tests under identical conditions and additional tests considering other condition combinations. Secondly, the experiments in this study were conducted based on the adoption of ARC, which shows a limitation in testing cells with a large nominal capacity. Though this study selected a relatively large-capacity battery (16 Ah), the TR behavior observed in this study may not be directly transferable to the large-format cells used in EV applications. It is believed that selecting larger-capacity cells can better reflect the intrinsic thermal behavior of LIBs in EVs, and thus help to characterize their degradation process and TR behavior. In addition, this study focuses more on cells than battery packs, and therefore lacks discussions about interactions between cells, such as the TR propagation, which has been considered to cause more severe safety consequences. Finally, due to the fact that discussions in this study are conducted based on the intrinsic thermal behavior of LIBs from experiments, the effectiveness of data-driven solutions in terms of TR risks of EVs have to be further validated through system-level and field studies. Several aspects are expected to be considered for the next steps, including impacts from external factors, the complexity of sensor deployment in practical scenarios, and the feasibility of integrating early warning capabilities into the current BMS. Moreover, considering the fact that real-world EV batteries may also operate under extreme temperature conditions, extending the temperature range in experiments is meaningful. These will greatly improve the applicability and reliability of data-driven safety management strategies during actual operations of EVs in different environments. Overall, future work will focus on further validating and developing applicable data-driven approaches, including expanding the sample size and temperature range through more experiments, conducting field tests, and developing effective techniques and algorithms to enable functions like anomaly detection, diagnosis, and even prognostics toward the TR risks of EVs, and thus instills more confidence in EV operations and decision-making processes, with the consideration of uncertainty and risks.

5. Conclusions

This study provides exploratory insights into data-driven approaches that may support safety management strategies for managing thermal runaway risks for electric vehicles. Intrinsic degradation patterns of lithium-ion batteries under adiabatic conditions have been explored in an experimental scenario, using an accelerating rate calorimeter. The results revealed the main characteristics in battery degradations through synergistically analyzing the thermal, electrochemical, and environmental parameters. These characteristics can support the exploration of thermal runaway precursors, the development of early warning

technologies, and consequently, the implementation of data-driven safety management strategies for EVs.

Author Contributions: Conceptualization, Y.X. (Yunli Xu), H.S., J.G., and M.D.; methodology, Y.X. (Yunli Xu), H.S.; software, Y.X. (Yunli Xu), J.Q., Y.X. (Yang Xu), and C.Z.; validation, H.S., J.G., and M.D.; formal analysis, H.S. and Y.X. (Yunli Xu); investigation, H.S. and Y.X. (Yunli Xu); resources, Y.X. (Yunli Xu); data curation, Y.X. (Yunli Xu), J.Q., Y.X. (Yang Xu), and C.Z.; writing—original draft preparation, H.S.; writing—review and editing, H.S., J.G., D.F., and M.D.; visualization, H.S.; supervision, D.F., M.D., and Y.X. (Yunli Xu); project administration, Y.X. (Yunli Xu); funding acquisition, Y.X. (Yunli Xu). All authors have read and agreed to the published version of the manuscript.

Funding: This research was funded by the Zhejiang Provincial Administration for Market Regulation's Eagle Plan Cultivation Major Project, "Risk assessment of thermal runaway in lithium-ion power batteries and research on modification of positive electrode materials", grant number CY2023105. This research was also funded by the Zhejiang Provincial Administration for Market Regulation's Science and Technology Project "Research on Safety Fault Identification, Cause Tracing, and Risk Control for Stacker-type Automated Warehouses in Industrial Product Manufacturing Enterprises", grant number ZD20240005.

Institutional Review Board Statement: Not applicable.

Informed Consent Statement: Not applicable.

Data Availability Statement: Data will be made available upon request.

Acknowledgments: This research was supported by the program of the China Scholarship Council (No. CSC202207930021).

Conflicts of Interest: The authors declare no conflicts of interest.

Abbreviations

The following abbreviations are used in this manuscript:

ARC	Accelerating Rate Calorimeter
BMS	Battery Management System
BTMS	Battery Thermal Management System
EVs	Electric Vehicles
HT	High Operating Temperature Condition
HWS	Heat–Wait–Search
LIBs	Lithium-ion Batteries
NCM	Nickel–Cobalt–Manganese
NT	Normal Operating Temperature Condition
SOC	State of Charge
SOH	State of Health
ROC	Rate of Change
TR	Thermal Runaway

References

1. Cicconi, P.; Landi, D.; Germani, M. Thermal Analysis and Simulation of a Li-Ion Battery Pack for a Lightweight Commercial EV. *Appl. Energy* **2017**, *192*, 159–177. [CrossRef]
2. BhaskaraRao, B.V.; Pabba, D.P.; Aepuru, R.; Akbari-Fakhrabadi, A.; Lokhande, P.; Udayabhaskar, R.; Rosales-Vera, M.; Espinoza-González, R. Fe_3O_4 nanoparticles intercalated reduced graphene oxide nanosheets for supercapacitor and lithium-ion battery anode performance. *J. Mater. Sci. Mater. Electron.* **2023**, *34*, 1910. [CrossRef]
3. Lokhande, P.E.; Misal, P.; Kalubarme, R.S.; Kulkarni, M.V.; Rednam, U.; Padlkar, S.; Al-Asbahi, B.A. Scalable microwave-assisted production of Ti_3C_2Tx MXene for next-generation Li-ion and Na-ion batteries. *Diam. Relat. Mater.* **2025**, *157*, 112503. [CrossRef]

4. Qi, C.; Liu, Z.; Lin, C.; Hu, Y.; Yan, T.; Zhou, Y.; Chen, B. Study on the Thermal Runaway Characteristics and Debris of Lithium-Ion Batteries under Overheating, Overcharge, and Extrusion. *J. Energy Storage* **2023**, *72*, 108821. [CrossRef]
5. Liang, X.; Wang, P.; Cao, X.; Wan, X.; Chao, P.; Zhao, X.; Yu, A.; Liu, C.; Li, J. Research on Improving the Safety of New Energy Vehicles Exploits Vehicle Operating Data. *Saf. Sci.* **2025**, *181*, 106681. [CrossRef]
6. Cui, H.; Wu, H.; He, D.; Ma, S. Noble Metal (Pd, Pt)-Functionalized WSe2 Monolayer for Adsorbing and Sensing Thermal Runaway Gases in LIBs: A First-Principles Investigation. *Environ. Res.* **2025**, *269*, 120847. [CrossRef] [PubMed]
7. Hu, D.; Huang, S.; Wen, Z.; Gu, X.; Lu, J. A Review on Thermal Runaway Warning Technology for Lithium-Ion Batteries. *Renew. Sustain. Energy Rev.* **2024**, *206*, 114882. [CrossRef]
8. Harper, G.; Sommerville, R.; Kendrick, E.; Driscoll, L.; Slater, P.; Stolkin, R.; Walton, A.; Christensen, P.; Heidrich, O.; Lambert, S.; et al. Recycling Lithium-Ion Batteries from Electric Vehicles. *Nature* **2019**, *575*, 75–86. [CrossRef] [PubMed]
9. Wang, Q.; Ping, P.; Zhao, X.; Chu, G.; Sun, J.; Chen, C. Thermal Runaway Caused Fire and Explosion of Lithium Ion Battery. *J. Power Sources* **2012**, *208*, 210–224. [CrossRef]
10. Feng, X.; Ouyang, M.; Liu, X.; Lu, L.; Xia, Y.; He, X. Thermal Runaway Mechanism of Lithium Ion Battery for Electric Vehicles: A Review. *Energy Storage Mater.* **2018**, *10*, 246–267. [CrossRef]
11. Feng, X.; Ren, D.; He, X.; Ouyang, M. Mitigating Thermal Runaway of Lithium-Ion Batteries. *Joule* **2020**, *4*, 743–770. [CrossRef]
12. Deng, J.; Bae, C.; Marcicki, J.; Masias, A.; Miller, T. Safety Modelling and Testing of Lithium-Ion Batteries in Electrified Vehicles. *Nat. Energy* **2018**, *3*, 261–266. [CrossRef]
13. Li, Y.; Chang, L.; Kong, L.; Zhao, X.; Zheng, J.; Wen, X.; Kou, G.; Mu, M. A Novel Cold Plate Battery Thermal Management System for NEDC and WLTC Driving Conditions. *Appl. Therm. Eng.* **2025**, *279*, 127874. [CrossRef]
14. Xiong, R.; Zhang, Y.; Wang, J.; He, H.; Peng, S.; Pecht, M. Lithium-Ion Battery Health Prognosis Based on a Real Battery Management System Used in Electric Vehicles. *IEEE Trans. Veh. Technol.* **2019**, *68*, 4110–4121. [CrossRef]
15. Saw, L.H.; Poon, H.M.; Thiam, H.S.; Cai, Z.; Chong, W.T.; Pambudi, N.A.; King, Y.J. Novel Thermal Management System Using Mist Cooling for Lithium-Ion Battery Packs. *Appl. Energy* **2018**, *223*, 146–158. [CrossRef]
16. Mashayekhi, M.; Houshfar, E.; Ashjaee, M. Development of Hybrid Cooling Method with PCM and Al_2O_3 Nanofluid in Aluminium Minichannels Using Heat Source Model of Li-Ion Batteries. *Appl. Therm. Eng.* **2020**, *178*, 115543. [CrossRef]
17. Yin, L.; Wei, R.; Zhang, L.; Chen, S.; Ren, Z.; Wang, Z.; Huang, S. Analysis of the Fire Evolution Process of an Electric Vehicle in a Confined Garage. *Tunn. Undergr. Space Technol.* **2026**, *167*, 107062. [CrossRef]
18. Lopez, C.F.; Jeevarajan, J.A.; Mukherjee, P.P. Experimental Analysis of Thermal Runaway and Propagation in Lithium-Ion Battery Modules. *J. Electrochem. Soc.* **2015**, *162*, A1905. [CrossRef]
19. Zhang, Q.; Liu, T.; Wang, Q. Experimental Study on the Influence of Different Heating Methods on Thermal Runaway of Lithium-Ion Battery. *J. Energy Storage* **2021**, *42*, 103063. [CrossRef]
20. Chen, K.; Luo, Y.; Long, Z.; Li, Y.; Nie, G.; Liu, K.; Xin, D.; Gao, G.; Wu, G. Big Data-Driven Prognostics and Health Management of Lithium-Ion Batteries:A Review. *Renew. Sustain. Energy Rev.* **2025**, *214*, 115522. [CrossRef]
21. Xie, Z.; Zhang, Y.; Wang, H.; Li, P.; Shi, J.; Zhang, X.; Li, S. The Multi-Parameter Fusion Early Warning Method for Lithium Battery Thermal Runaway Based on Cloud Model and Dempster–Shafer Evidence Theory. *Batteries* **2024**, *10*, 325. [CrossRef]
22. Wei, N.; Zhang, F.; Zhang, W.; Li, X. Comparative Study on the Thermal Runaway Characteristics of Li(NixCoyMnz)O2 Batteries. *Heliyon* **2024**, *10*, e31203. [CrossRef]
23. Abdolrasol, M.G.M.; Ayob, A.; Lipu, M.S.H.; Ansari, S.; Kiong, T.S.; Saad, M.H.M.; Ustun, T.S.; Kalam, A. Advanced Data-Driven Fault Diagnosis in Lithium-Ion Battery Management Systems for Electric Vehicles: Progress, Challenges, and Future Perspectives. *eTransportation* **2024**, *22*, 100374. [CrossRef]
24. Teng, Z.; Lv, C. Detection toward Early-Stage Thermal Runaway Gases of Li-Ion Battery by Semiconductor Sensor. *Front. Chem.* **2025**, *13*, 1586903. [CrossRef]
25. Han, D.; Wang, J.; Yin, C.; Zhao, Y. Advances in Early Warning of Thermal Runaway in Lithium-Ion Battery Energy Storage Systems. *Adv. Sens. Res.* **2025**, *4*, 2400165. [CrossRef]
26. Balakrishnan, P.G.; Ramesh, R.; Prem Kumar, T. Safety Mechanisms in Lithium-Ion Batteries. *J. Power Sources* **2006**, *155*, 401–414. [CrossRef]
27. Gabbar, H.A.; Othman, A.M.; Abdussami, M.R. Review of Battery Management Systems (BMS) Development and Industrial Standards. *Technologies* **2021**, *9*, 28. [CrossRef]
28. Lu, L.; Han, X.; Li, J.; Hua, J.; Ouyang, M. A Review on the Key Issues for Lithium-Ion Battery Management in Electric Vehicles. *J. Power Sources* **2013**, *226*, 272–288. [CrossRef]
29. Waseem, M.; Ahmad, M.; Parveen, A.; Suhaib, M. Battery Technologies and Functionality of Battery Management System for EVs: Current Status, Key Challenges, and Future Prospectives. *J. Power Sources* **2023**, *580*, 233349. [CrossRef]
30. Tran, M.-K.; Panchal, S.; Khang, T.D.; Panchal, K.; Fraser, R.; Fowler, M. Concept Review of a Cloud-Based Smart Battery Management System for Lithium-Ion Batteries: Feasibility, Logistics, and Functionality. *Batteries* **2022**, *8*, 19. [CrossRef]

31. Jaguemont, J.; Boulon, L.; Dubé, Y.; Martel, F. Thermal Management of a Hybrid Electric Vehicle in Cold Weather. *IEEE Trans. Energy Convers.* **2016**, *31*, 1110–1120. [CrossRef]
32. Abdelkareem, M.A.; Maghrabie, H.M.; Abo-Khalil, A.G.; Adhari, O.H.K.; Sayed, E.T.; Radwan, A.; Rezk, H.; Jouhara, H.; Olabi, A.G. Thermal Management Systems Based on Heat Pipes for Batteries in EVs/HEVs. *J. Energy Storage* **2022**, *51*, 104384. [CrossRef]
33. Gasmelseed, A.; Ismael, M.A.; Said, M.A.; Ahmad, F.; Osman, S. Thermal Management Strategies for Lithium-Ion Batteries in Electric Vehicles: A Comprehensive Review of Nanofluid-Based Battery Thermal Management Systems. *Results Eng.* **2024**, *24*, 103339. [CrossRef]
34. Wu, W.; Wang, S.; Wu, W.; Chen, K.; Hong, S.; Lai, Y. A Critical Review of Battery Thermal Performance and Liquid Based Battery Thermal Management. *Energy Convers. Manag.* **2019**, *182*, 262–281. [CrossRef]
35. Yang, J.; Hong, J.; Zhang, X.; Du, Y.; Hou, Y.; Chen, Y.; Wang, F.; Chen, Y.; Wang, H. Thermal Runaway Classification and Early Warning for Lithium-Ion Batteries Based on Voltage Feature Statistics and Multi-Model Fusion. *Appl. Therm. Eng.* **2025**, *280*, 128075. [CrossRef]
36. Hu, X.; Feng, F.; Liu, K.; Zhang, L.; Xie, J.; Liu, B. State Estimation for Advanced Battery Management: Key Challenges and Future Trends. *Renew. Sustain. Energy Rev.* **2019**, *114*, 109334. [CrossRef]
37. Gnanaraj, J.S.; Zinigrad, E.; Asraf, L.; Gottlieb, H.E.; Sprecher, M.; Aurbach, D.; Schmidt, M. The Use of Accelerating Rate Calorimetry (ARC) for the Study of the Thermal Reactions of Li-Ion Battery Electrolyte Solutions. *J. Power Sources* **2003**, *119–121*, 794–798. [CrossRef]
38. Yue, Y.; Jia, Z.; Li, Y.; Wen, Y.; Lei, Q.; Duan, Q.; Sun, J.; Wang, Q. Thermal Runaway Hazards Comparison between Sodium-Ion and Lithium-Ion Batteries Using Accelerating Rate Calorimetry. *Process Saf. Environ. Prot.* **2024**, *189*, 61–70. [CrossRef]
39. Lei, B.; Zhao, W.; Ziebert, C.; Uhlmann, N.; Rohde, M.; Seifert, H.J. Experimental Analysis of Thermal Runaway in 18650 Cylindrical Li-Ion Cells Using an Accelerating Rate Calorimeter. *Batteries* **2017**, *3*, 14. [CrossRef]
40. Zhang, Y.; Li, Y.; Jia, Z.; Liu, Y.; Yu, Y.; Jiang, L.; Wang, Q.; Duan, Q.; Sun, J. Investigating the Safety of Solid/Liquid Hybrid Electrolyte Lithium-Ion Battery: A Comparative Study with Traditional LIBs under Abuse Condition. *J. Power Sources* **2024**, *620*, 235261. [CrossRef]
41. Liu, F.; Hu, Q.; Jiang, C.; Xu, Y.; Yan, P.; Sui, X. The Suppression Performance of Fluorinated Cooling Agents on the Lithium-Ion Batteries Fire Based on the Accelerating Rate Calorimeter (ARC). *Therm. Sci. Eng. Prog.* **2023**, *42*, 101877. [CrossRef]
42. Kim, S.W.; Lee, E.J. A Comparative Experimental Study between Cone Calorimeter and Accelerating Rate Calorimeter for Lithium Ion Battery Fires. *Appl. Therm. Eng.* **2025**, *279*, 127857. [CrossRef]
43. Ding, J.; Liu, K.; Xu, C.; Li, J.; Yan, X.; Liang, J.; Feng, M.; Kossoy, A.A.; Xu, J.; Hu, D. Accelerating Rate Calorimetry: History, State of the Art and Perspectives. *Chem. Thermodyn. Therm. Anal.* **2025**, *18*, 100182. [CrossRef]
44. Ouyang, D.; Chen, M.; Weng, J.; Wang, K.; Wang, J.; Wang, Z. Exploring the Thermal Stability of Lithium-Ion Cells via Accelerating Rate Calorimetry: A Review. *J. Energy Chem.* **2023**, *81*, 543–573. [CrossRef]
45. Feng, X.; Fang, M.; He, X.; Ouyang, M.; Lu, L.; Wang, H.; Zhang, M. Thermal Runaway Features of Large Format Prismatic Lithium Ion Battery Using Extended Volume Accelerating Rate Calorimetry. *J. Power Sources* **2014**, *255*, 294–301. [CrossRef]
46. Wei, Z.; Peng, Y.; Yuan, Q.; Chen, J.; Hou, B.; Huang, K.; Meng, H.; Xu, C.; Chen, M.; Feng, X.; et al. A Novel Self-Adaptive Microcapsule Mitigating the Thermal Runaway Hazards of Lithium-Ion Batteries. *J. Energy Storage* **2025**, *136*, 118238. [CrossRef]